Pharmacological Research - Natural Products 8 (2025) 100361

Contents lists available at ScienceDirect

Pharmacological Research - Natural Products

journal homepage: www.sciencedirect.com/journal/prenap

Anemonin is one of two anti-mitotic activities present in extracts from the Canadian Prairie Crocus, *Pulsatilla nuttalliana*

Shannon M. Healy Knibb [a], Tanner C. Lockwood [a], Benjamin Yeremy [b], Layla Molina [a], Chad R. Beck [a], Araba Sagoe-Wagner [a], David E. Williams [b], Raymond J. Andersen [b], Roy M. Golsteyn [a,*]

[a] Natural Product Laboratory, University of Lethbridge, 4401 University Drive W, Lethbridge, AB T1K 3M4, Canada
[b] Departments of Chemistry and EOAS, University of British Columbia, 2036 Main Mall, Vancouver, BC V6T 1Z1, Canada

ARTICLE INFO

Keywords:
Anemone
Canada
Mitosis
Mitotic spindle
Ranunculaceae

ABSTRACT

We are investigating plants from the prairie ecological zone of Canada to identify natural products that inhibit mitosis in cancer cells. Extracts prepared from the Canadian prairie plant species *Pulsatilla nuttalliana* (Ranunculaceae) exhibited anti-mitotic activity on human cancer cell lines. *P. nuttalliana*-treated cells acquired a rounded morphology and were positive for phospho-histone H3, a mitotic protein. Further investigation revealed that some arrested cells displayed mitotic spindles, whereas others lacked detectable spindles. Fractionation of the extract prepared from plant stems revealed two distinct anti-mitotic activities, each of which exhibited different effects on spindle organization. Using biology-guided fractionation, we isolated one of the anti-mitotic compounds as the natural product anemonin and are the first to report its anti-mitotic activity. In addition, this is the first report of two distinct anti-mitotic activities in one botanical species and contributes to a growing body of evidence that select Canadian prairie plants have a range of anti-mitotic activities.

1. Introduction

The investigation of natural products contributes to the advancement of new chemical compounds for treating diseases such as cancer. We are investigating natural products from Canadian botanical species that interfere with the cell division cycle in human cells. A classic example is paclitaxel, a taxane compound isolated from *Taxus brevifolia*, which binds to tubulin resulting in the arrest of cells in mitosis [1,2]. The study of paclitaxel, also known as Taxol®, has provided detailed information about tubulin function and it has become one of the most widely used chemotherapeutic drugs to treat cancer [3–5]. Despite such discoveries, the potential of natural products from botanicals in Canadian ecological zones as scientific tools or medicines remains underexplored [6,7].

An important element in the discovery of natural product inhibitors is the choice of sources from which to find such compounds [8]. We focus on investigating plant species from the prairie ecological zone in Canada because these plants grow under conditions that promote the production of secondary metabolites [7,9,10]. The combination of biotic conditions, such as herbivory, and abiotic conditions, such as extreme temperature ranges, may contribute to the production of either abundant or novel secondary metabolites [11,12]. In the province of Alberta, Canada, which harbours prairie and montane ecological zones, 1636 vascular plant species from 123 botanical families have been catalogued [13]. The secondary metabolite activities of many of these plant species are unknown, presenting an avenue for further exploration.

The second component of identifying natural product inhibitors is the bio-assay. We utilized phenotypic assays, which favour the discovery of novel inhibitory activities because an entire biochemical pathway can be tested at once [14,15]. This complements assays using purified systems, such as protein kinases, for which the precise target is known [16,17]. We developed a cell-based assay for the detection of mitosis in HT-29 cells, which are particularly sensitive to mitotic arrest [18], in which the phenotype is the acquisition of a rounded morphology that is characteristic of mitosis [19,20]. Identification of the molecular target

Abbreviations: β-ME, beta-mercaptoethanol; BSA, bovine serum albumin; DAPI, 4′,6-diamidino-2-phenylindole; DCM, dichloromethane; DMSO, dimethyl sulfoxide; DPT, 4-deoxypodophyllotoxin; EtOH, ethanol; H, hour; Min, minute; MTT, 3–4,5-dimethylthiazol-2-yl-2,5-diphenyltetrazolium; NT, not-treated; PBS, phosphate buffered saline; PH3, phospho-histone H3; V, volume.

* Correspondence to: Natural Product Laboratory, Department of Biological Sciences, University of Lethbridge, Lethbridge, AB T1K 3M4, Canada.
E-mail address: roy.golsteyn@uleth.ca (R.M. Golsteyn).

https://doi.org/10.1016/j.prenap.2025.100361
Received 21 March 2025; Received in revised form 12 August 2025; Accepted 1 September 2025
Available online 3 September 2025

requires additional study; however, the phenotypic approach is a critical first step that has successfully led to the purification and identification of inhibitory compounds [21–24].

We created an extract library prepared from Canadian plant species and screened it using phenotypic assays for extracts that induced a mitotic arrest [7]. Here, we report the characterization of an anti-mitotic activity of extracts prepared from the Prairie Crocus, *Pulsatilla nuttalliana* (Ranunculaceae; previously Anemone), a prominent spring prairie plant [25]. A species related to *P. nuttalliana*, *P. koreana*, is known to Korean Traditional knowledge [26] and is a source of deoxypodophyllotoxin, a tubulin toxin that arrests cells in mitosis [27]. We are the first to investigate *P. nuttalliana*, whose distribution is limited to North America. By combining phenotypic assays with specific tests for mitotic function, we found that there were not one, but two distinct anti-mitotic activities present in this species. This is the first report of two distinct anti-mitotic activities in extracts from one botanical species.

2. Materials and methods

2.1. Plant collection

Aerial plant parts of *P. nuttalliana* (Ranunculaceae) were collected by sustainable practice in southern Alberta, Canada at North 49°1 latitude and West −113°0 longitude, at approximately 850–1400 m elevation during the years 2015 and 2019. Permits from provincial and local governments were acquired for collection. Plant taxonomy was confirmed to species [13,28] and verified by the University of Lethbridge Herbarium. A voucher specimen was provided to the herbarium as #Golsteyn080. Following harvest, the plants were dried at room temperature and stored in the dark in a dry environment at room temperature until extraction.

2.2. Preparation of plant extracts

Plant parts (whole aerial plant parts, leaves, stems, and flowers) were separated and ground into fine powders. Extracts were prepared by suspending powdered material in either 75 % (v/v) ethanol in water (A extracts) or in 100 % dichloromethane (B extracts) and stirring overnight at room temperature. The suspensions were filtered, dried, and stored in the dark at room temperature. Whole plant extracts were given the codes PP820A and PP820B, extracts from leaves were given the codes PP1630A and PP1630B, extracts from stems were given the codes PP1631A and PP1631B, and extracts from flowers were given the codes PP1632A and PP1632B. The extracts were dissolved in dimethyl sulfoxide (DMSO) (Sigma-Aldrich, D2438) to a concentration of 50 mg/mL for use in biological assays.

2.3. Cell culture

The human cell lines HT-29 (ATCC HTB-38) and U2OS (ATCC HTB-96) were obtained from the American Type Culture Collection (ATCC) and cultivated as previously described [19,29]. HT-29 cells were plated at a density of 3.0×10^5 cells/25 cm^2 flask and cultured for 48 h prior to treatment. U2OS cells were plated at a density of 3.0×10^5 cells/25 cm^2 flask and cultured for 24 h prior to treatment. The compounds nocodazole (660 μM, Sigma-Aldrich, M1404), paclitaxel (1 mM, Sigma, T7402), 4-deoxypodophyllotoxin (125 μM, Cedarlane, D249500), hymenoratin (3.8 mM) and anemonin (10 mM, Millipore Sigma, PHL80346) were dissolved in DMSO and stored at −20°C. For not-treated cells, DMSO was added at a final concentration of 0.4 % (v/v) as a solvent vehicle control. Light microscopy imaging was performed with an Infinity 1 camera operated by Infinity Capture imaging software (Lumenera Corporation, CA) on an Olympus CKX41 inverted microscope. Cells were manually scored for rounded or flat morphology. At least 200 cells were counted per treatment group.

2.4. Cell viability (MTT) assay

The 3-(4,5-dimethylthiazol-2-yl)-2,5-diphenyltetrazolium (MTT) assay (Sigma-Aldrich, M2128–1G) was used to measure plant extract cytotoxicity [19]. HT-29 cells were seeded at 5000 cells per well in a 96-well culture plate and incubated at 37°C for 48 h prior to treatment. All experiments were carried out in triplicate, and the treatments were repeated at least three times. After 72 h of treatment, 20 μL of MTT solution (5 mg/mL MTT in phosphate-buffered saline (PBS: 137 mM NaCl, 3 mM KCl, 100 mM Na_2HPO_4, 18 mM KH_2PO_4)) was added to the medium in each well, and the plates were incubated at 37°C for 3.5 h. The medium was then aspirated and replaced with 150 μL of MTT solvent (4 mM HCl, 0.1 % (v/v) octylphenoxypolyethoxyethanol, in isopropanol) in each well. The plates were left in the dark for 15 min with shaking, and a Cytation™ 5 Cell Imaging Multi-Mode Reader (BioTek Instruments, USA) equipped with Gen5 software was used to measure the absorbance at 590 nm. IC_{50} concentrations were calculated as the concentration of the compound or plant extract that reduced the absorbance of MTT by 50 % compared to 0.1 % (v/v) DMSO-treated cells. The normalized percent absorbance was calculated as follows:

Normalized percent absorbance = (absorbance/DMSO absorbance) x 100

The log concentrations of the compounds were plotted against the normalized absorbance percentage using Microsoft Excel. Analysis was performed with GraphPad Prism 5 software, using non-linear regression (log(inhibitor) versus normalized response) to estimate IC_{50} concentrations. Standard curves were plotted using the following equation:

$Y = \text{maximum} + (\text{maximum} - \text{minimum}) / (1 + 10(X\text{-}\text{Log}IC_{50}))$

Where Y is the percentage of viable cells, maximum is the percentage of viable cells after treatment with 0.1 % DMSO, minimum is the percentage of viable cells after treatment with the highest concentration of the cytotoxic compound, and X is the $\log_{10}$ value of the treatment concentration.

2.5. Immunofluorescence microscopy

HT-29 cells were seeded in 6 well culture plates on glass coverslips and incubated at 37°C for 48 h prior to treatment. After 18 h of treatment, the cells were fixed for 20 min at room temperature with 3 % (v/v) paraformaldehyde (Fisher Scientific, 30525–89–4) in PBS. Fixation was halted with 50 mM NH_4Cl in PBS for 10 min, and then cells were permeabilized for 5 min with 0.2 % (v/v) Triton X-100 in PBS and blocked with 3 % (w/v) bovine serum albumin (BSA) in PBS-T (0.1 % (v/v) Tween 20 diluted in PBS) for 30 min. Cells were then incubated overnight at 4°C with primary antibodies anti-phospho-Ser10 histone H3 (Millipore, 06–570(CH); 1:1000) and anti-α-tubulin (Santa Cruz Biotechnology, sc-53030; 1:400). After incubation, cells were washed with PBS-T and incubated with secondary antibodies Alexa Fluor 594 AffiniPure goat anti-rabbit IgG (Jackson ImmunoResearch, 111–585–003; 1:300) and Alexa Fluor 488 rabbit anti-rat IgG (ThermoFisher, A11006; 1:200) for 45 min at room temperature. Nuclei were stained with 300 nM 4′,6-diamidino-2-phenylindole (DAPI) (Fisher, LSD1306) in PBS for 15 min. After staining, the coverslips were mounted onto microscope slides with ProLong Gold Antifade Mountant (Thermo Fisher; P36934). Cells were then observed and imaged with a Cytation™ 5 Cell Imaging Multi-Mode Reader using the Gen5 software (BioTek Instruments, USA) and a Zeiss Axio Observer Z1 Motorized Inverted Fluorescence Microscope using AxioVision software (ZEISS, USA). A minimum of 200 cells were counted for each treatment, and the mean percentage and standard error of the mean of PH3-positive cells in at least three independent experiments were calculated. DMSO-treated mitotic cells were used as a reference for baseline mitotic spindle morphology.

2.6. Spectrophotometry

The extracts and fractions were diluted to 1 mg/mL in 100 % methanol, and 75 µL of each sample was transferred to separate wells of a 96 well plate. The absorbance of each well was read on an Epoch microplate spectrophotometer (BioTek Instruments, USA) from 300 to 700 nm, with steps of 2 nm between reads. Absorbance data were blanked to a methanol negative control and normalized using the following equation:

Normalized absorbance = (absorbance - minimum) / (maximum - minimum)

2.7. Cell cycle analysis

HT-29 cells were plated at 3.0×10^5 cells/25 cm^2 flask and incubated at 37°C for 48 h prior to treatment for 18 h. Treated cells were collected by trypsinization, washed with cold PBS (0.8 % FBS (fetal bovine serum), 1 mM EDTA (ethylenediaminetetraacetic acid)), and fixed in ice-cold 70 % ethanol for 24 h. The fixed samples were stored at −20°C until use. For analysis, the samples were centrifuged at 300 × *g* for 5 min at 4°C, washed with PBS at room temperature, and resuspended in Muse® Cell Cycle staining reagent. The cells were incubated for 30 min and analyzed using a Muse® Cell Analyzer (Luminex). Gating was set using a not-treated sample and experiments were performed three times.

2.8. LH-20 column chromatography

The extract PP1631A was subjected to column chromatography in which 200 µL of a 100 mg/mL solution of PP1631A in 100 % methanol was loaded onto a Sephadex LH-20 column (225 mm length × 15 mm internal diameter) pre-equilibrated with 100 % methanol. The column was then eluted with 100 % methanol, yielding twelve 2 mL fractions (including a void volume fraction). The fractions were evaporated under vacuum and resuspended in 100 % methanol to a concentration of 10 µg/mL.

2.9. Beta-mercaptoethanol reduction assay

HT-29 cells were either treated with nocodazole, 4-deoxypodophyllotoxin, hymenoratin, fraction 2, fraction 5, or anemonin alone, or treated in combination with beta-mercaptoethanol (β-ME) (MP BioMedical, 02194705-CF). Each compound was preincubated with 0.1 mM β-ME for 1 h at 37°C prior to addition to media for cell culture treatment. After 18 h of treatment, light microscopy images were taken as described above.

2.10. Biology-guided fractionation and isolation of anemonin

2.10.1. General experimental procedures

The ^1H and ^{13}C NMR spectra were recorded on a Bruker AV-500 spectrometer with a 5 mm CPTCI cryoprobe. ^1H chemical shifts are referenced to the residual DMSO-d_6 (δ 2.49 ppm) and ^{13}C chemical shifts are referenced to the DMSO-d_6 solvent peak in the literature (δ 39.5 ppm) [30]. Merck Type 5554 silica gel plates were used for analytical thin layer chromatography. Low- and high-resolution ESI--QIT-MS were recorded on a Bruker-Hewlett Packard 1100 Esquire–LC system mass spectrometer. Reversed-phase HPLC purifications were performed on a Waters 1525 Binary HPLC pump attached to a Waters 2998 Photodiode Array Detector. All solvents used for HPLC were Fisher HPLC grade.

2.10.2. Isolation of anemonin

Approximately 40 g of dried plant material was extracted twice with 200 mL methanol overnight at room temperature. The combined extracts were concentrated *in vacuo* and then taken up into 2:1 methanol: water and extracted 4 times with 100 mL of dichloromethane. The combined dichloromethane extracts were concentrated *in vacuo* to give 380 mg of extract. Approximately 1/4 of the active dichloromethane soluble material was chromatographed on Sephadex LH20 using a 71 × 2.5 cm column with methanol as eluent. The fractions obtained were labelled RA205–241 and analyzed with the cell rounding assay. The bioactive fraction obtained was then purified by C_{18} reversed-phase HPLC using an InertSustain, 5 µm, 25 × 1.0 cm column with a gradient transitioning over 60 min from 95 % H_2O/acetonitrile to 5 % H_2O/acetonitrile as eluent with a flow rate of 2 mL/min to give 0.4 mg of anemonin (RA223). The structure of anemonin was confirmed by high-resolution electrospray ionization mass spectrometry (HRESIMS), analysis of standard 1D and 2D Nuclear Magnetic Resonance (NMR) spectra, and comparison with the literature values [30].

2.11. Statistical analysis

Data were analyzed using Microsoft Excel 2016 and GraphPad Prism 5. Data were plotted as the mean of three independent experiments ± standard error of the mean. One-way analysis of variance (ANOVA) with Tukey's post hoc test was used to analyze the results from the light microscopy and immunofluorescence microscopy assays. Differences were considered statistically significant when $p < 0.05$.

3. Results

3.1. Extracts prepared from Pulsatilla nuttalliana induced a mitotic arrest in cancer cells

Pulsatilla nuttalliana (Ranunculaceae), commonly known as the Prairie Crocus, is a prominent herbaceous plant in the prairie ecological system. It is one of the first plant species to emerge after winter, producing striking flowers before developing prominent leaves and stems approximately one month later (Fig. 1A). We extracted the aerial parts of *P. nuttalliana* from post-flowering plants with either 75 % ethanol (v/v) in water or 100 % dichloromethane and analyzed their absorbance by spectrophotometry over a range of wavelengths. The ethanolic extract absorbance was highest at 330 nm, whereas the DCM extract absorbance was highest at 410 nm, demonstrating that each extraction likely contained a different chemical mixture (Fig. 1B). We examined the properties of these extracts by adding them to the culture media of two cell lines (HT-29, Fig. 1C; U2OS, Fig. 1D). Cells were either not-treated, treated with nocodazole as a positive control for mitotic cell rounding, or treated with extracts at a concentration of 50 µg/mL for 18 h and observed by light microscopy. Few rounded cells were observed in the not-treated sample, whereas treatment with nocodazole induced cell rounding, indicative of mitosis. The ethanolic and DCM extracts of *P. nuttalliana* induced cell rounding in both HT-29 and U2OS cells. Additionally, we tested extracts prepared from *P. nuttalliana* collected at two different sites in southern Alberta and from plants collected in different years. We found that extracts from all collections induced the rounded morphology (data not shown). The *P. nuttalliana* extracts were subjected to further investigation to determine whether the cell rounding activity was caused by a mitotic arrest.

We tested extracts prepared from different plant parts of *P. nuttalliana* to characterize the cell rounding activity. Extracts were prepared from leaves, stems, or flowers using either 75 % (v/v) ethanol (labelled as A) or 100 % DCM (labelled as B). HT-29 cells were either not-treated, treated with nocodazole, or treated with concentrations of each extract ranging from 15 to 500 µg/mL for 18 h and observed by light microscopy (Fig. 2A). As expected, the not-treated cells had few rounded cells, whereas nocodazole induced nearly 100 % cell rounding. Imaging (Fig. 2A) and counting (Fig. 2B) revealed that all extracts induced cell rounding, although at different concentrations. The stem fractions induced cell rounding at the lowest concentrations of any plant part: there were 50 ± 1 % rounded cells at 150 µg/mL induced by ethanolic extraction and 81 ± 4 % rounded cells at 50 µg/mL induced by DCM extraction.

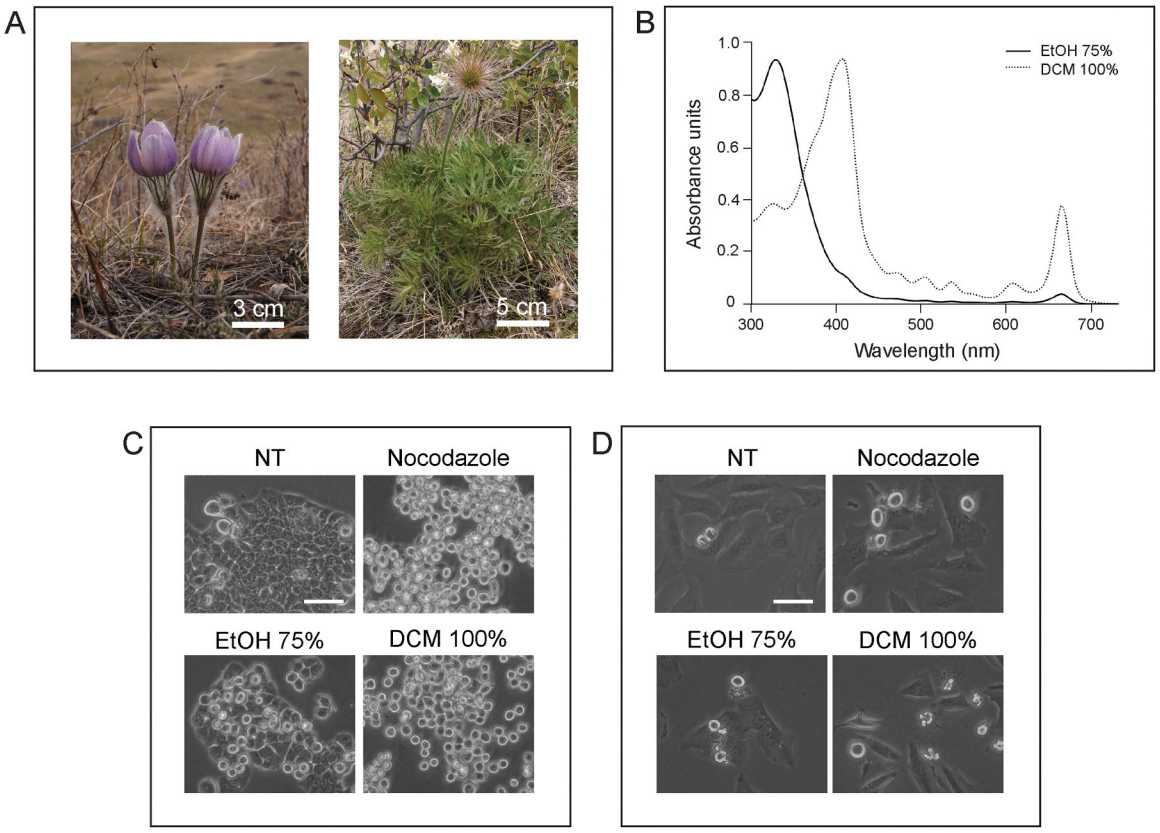

Fig. 1. HT-29 and U2OS cells treated with *Pulsatilla nuttalliana* ethanolic and dichloromethane whole plant extracts acquire a rounded morphology. **A.** *Pulsatilla nuttalliana* (Ranunculaceae) in prairie habitat. Flowers (left); leaves and stems (right). **B.** UV/visible absorbance spectra of *P. nuttalliana* ethanolic (EtOH, solid line) and dichloromethane (DCM, dotted line) whole plant extracts. **C.** HT-29 cells and **D.** U2OS cells were either not-treated, treated with 500 nM nocodazole, or treated with 50 μg/mL EtOH or DCM extracts for 18 h. Images were taken by light microscopy and representative images are shown. Scale bar represents 50 μm.

We investigated *P. nuttalliana* stem extracts in more detail because they exhibited cell rounding activity at the lowest concentration of all the extracts tested. Analysis by spectrophotometric absorbance readily distinguished the two stems extracts (Fig. 3A), with stems A absorbing more strongly below 400 nm and less strongly at 670 nm than stems B. The two extracts were tested for toxicity in HT-29 cells using the MTT assay (Fig. 3B). Stems A had an IC_{50} of 47 ± 15 μg/mL and stems B had an IC_{50} of 15 ± 5 μg/mL, which demonstrated that both extracts were moderately cytotoxic in addition to the cell-rounding activity. We noted that the values of cell viability for stems A were not easily fitted to a curve, which may reflect the activity described in later experiments. We next examined HT-29 cells by flow cytometry after treatment with stems A and stems B extracts to determine whether they underwent a cell cycle arrest, which would be consistent with the cell rounding effect. In a representative experiment, the number of cells with 4 N DNA at 18 h was 26 ± 1 % in not-treated cells and 94 ± 2 % in nocodazole-treated cells, as expected (Fig. 3C). Stems A- and stems B-treated cells showed similar 4 N DNA profiles of 67 ± 2 % and 71 ± 1 %, respectively. These data demonstrated that the two stem extracts were cytotoxic and caused cell cycle arrest.

To determine whether the cell rounding induced by *P. nuttalliana* extracts was caused by an arrest in mitosis, we used immunofluorescence microscopy to detect nuclei, the mitotic protein phospho-histone H3 (PH3), and the spindle protein tubulin (Fig. 4A). Cells were either not-treated or treated with nocodazole, paclitaxel, stems A or stems B extracts. The not-treated cells had relatively few nuclei stained positive for PH3, whereas the nuclei in cells treated with either nocodazole or paclitaxel were nearly all positive for PH3, as expected. Importantly, both extract treatments induced a PH3 signal, whereby stems A induced 47 ± 2 % of cells with a PH3 signal and stem B induced 83 ± 3 % of cells with a PH3 signal (Fig. 4B), supporting the evidence that cell rounding was linked to an arrest in mitosis.

3.2. *Pulsatilla nuttalliana extracts induced two distinct mitotic arrest phenotypes*

We then observed the organization of tubulin in mitotic cells treated with each extract using immunofluorescence microscopy (Fig. 4A). The few mitotic cells in the not-treated population showed bipolar spindles and these cells were co-stained with PH3 signals. Nocodazole prevents the formation of the mitotic spindle, leaving little or punctate staining, whereas paclitaxel stabilizes tubulin in spindle fibers, which increases signal intensity and co-localizes with PH3 signals. In cells treated with stems A, we made a striking observation of PH3-positive cells in which some contained tubulin spindle structures, whereas others did not. In contrast, stems B-treated mitotic cells did not contain spindles. We then calculated the percentage of cells in mitosis relative to the total population, and of those in mitosis, the percentage of cells that had a mitotic spindle (Fig. 4B). The non-treated sample had 5 ± 1 % of the cells in mitosis, of which 53 ± 2 % contained bipolar spindle organization, which is consistent with the mitotic phases (prophase to telophase). None of the nocodazole-treated cells contained a spindle structure, whereas all the paclitaxel-treated cells had a spindle structure, as expected. The stems A-treated mitotic cells showed 46 ± 4 % with a spindle structure, and the remainder had no organized tubulin structures. In contrast, only 1 % of the stems B mitotic cells contained a spindle structure.

We then explored the possibility that the stems A extract might contain two distinct anti-mitotic activities by applying column chromatography. The stems A extract was fractionated by LH-20 column

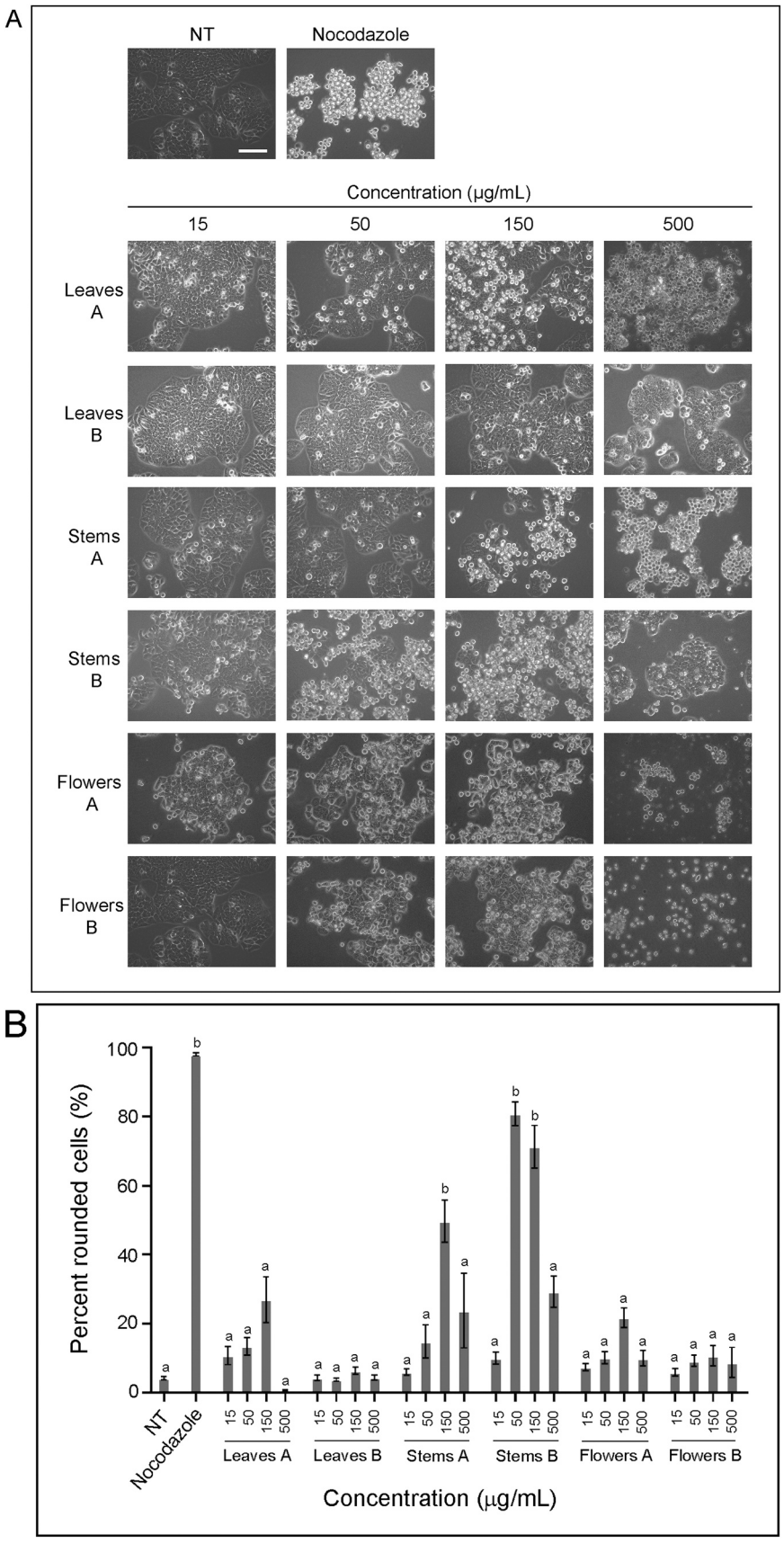

(caption on next page)

Fig. 2. HT-29 cells treated with ethanolic or dichloromethane extracts of *P. nuttalliana* leaves, stems, or flowers acquire a rounded morphology. **A.** HT-29 cells were either not-treated or treated with 500 nM nocodazole, *P. nuttalliana* ethanolic extracts (labelled as A) or dichloromethane extracts (labelled as B) of leaves, stems, or flowers for 18 h. Images were taken by light microscopy and representative images are shown. Scale bar represents 100 μm. **B.** The mean percentages of cells exhibiting a rounded morphology after treatment. Error bars represent the SEM of at least three independent experiments. Statistical significance was determined using one-way ANOVA followed by Tukey's post hoc test ($p < 0.0001$). Means that are significantly different from the mean of the not-treated control are represented with a different letter (a, b).

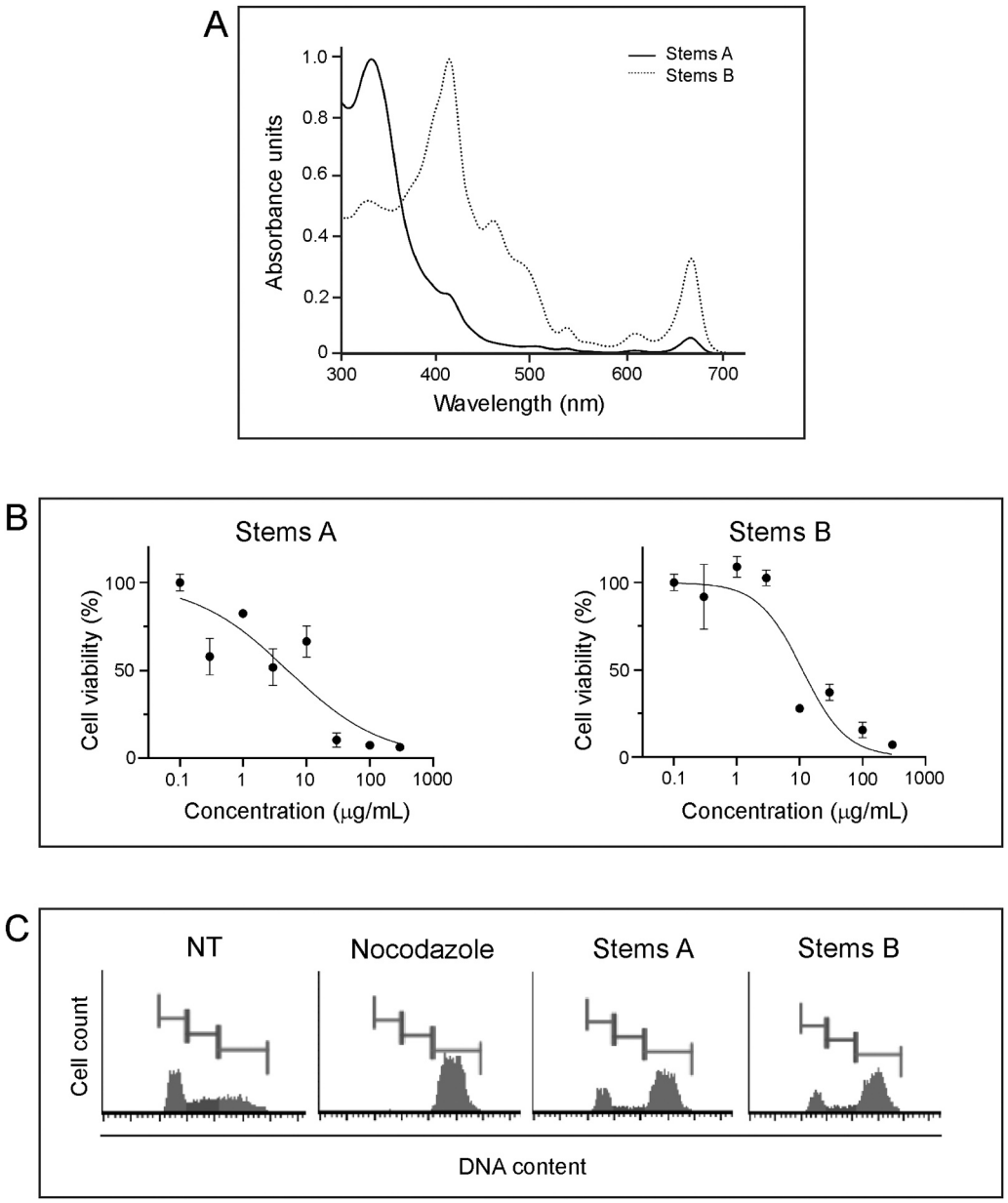

Fig. 3. Plant extracts stems A and stems B are both moderately cytotoxic and cause a cell cycle arrest associated with the G2/M phase. **A.** UV/visible absorbance spectra of stems A (solid line) and stems B (dotted line). **B.** Percent cell viability of HT-29 cells was plotted as a function of the extract treatment concentration. **C.** HT-29 cells were either not-treated or treated with 500 nM nocodazole, 150 μg/mL stems A or 50 μg/mL stems B and prepared for cell cycle analysis by flow cytometry. Histograms of representative experiments are shown with DNA content along the x-axis and cell count along the y-axis.

chromatography, yielding 12 fractions (including a void volume fraction). Cells were then either not-treated or treated with nocodazole, stems A, or a column fraction. After 18 h, the cells were observed by microscopy for cell rounding (Fig. 5A). Not-treated cells had relatively few rounded cells, whereas treatment with nocodazole or stems A extract induced many rounded cells, as expected. Prominent cell rounding effects were observed in fractions 1 through 5 inclusive, and not in the void volume or fractions 6 through 11. Fraction 2 and fraction 5 were selected for further investigation because they were chromatographically distant while still inducing cell rounding. We compared stems A, fraction 2, and fraction 5 by spectrophotometry and observed distinct spectra, suggesting that different compounds were eluted in each fraction (Fig. 5B). We then tested whether fraction 2 or fraction 5 induced either of the two types of spindle profiles (spindle or no spindle) that were observed in the stems A whole extract again utilizing immunofluorescence microscopy (Fig. 5C). Both fraction 2- and fraction 5-

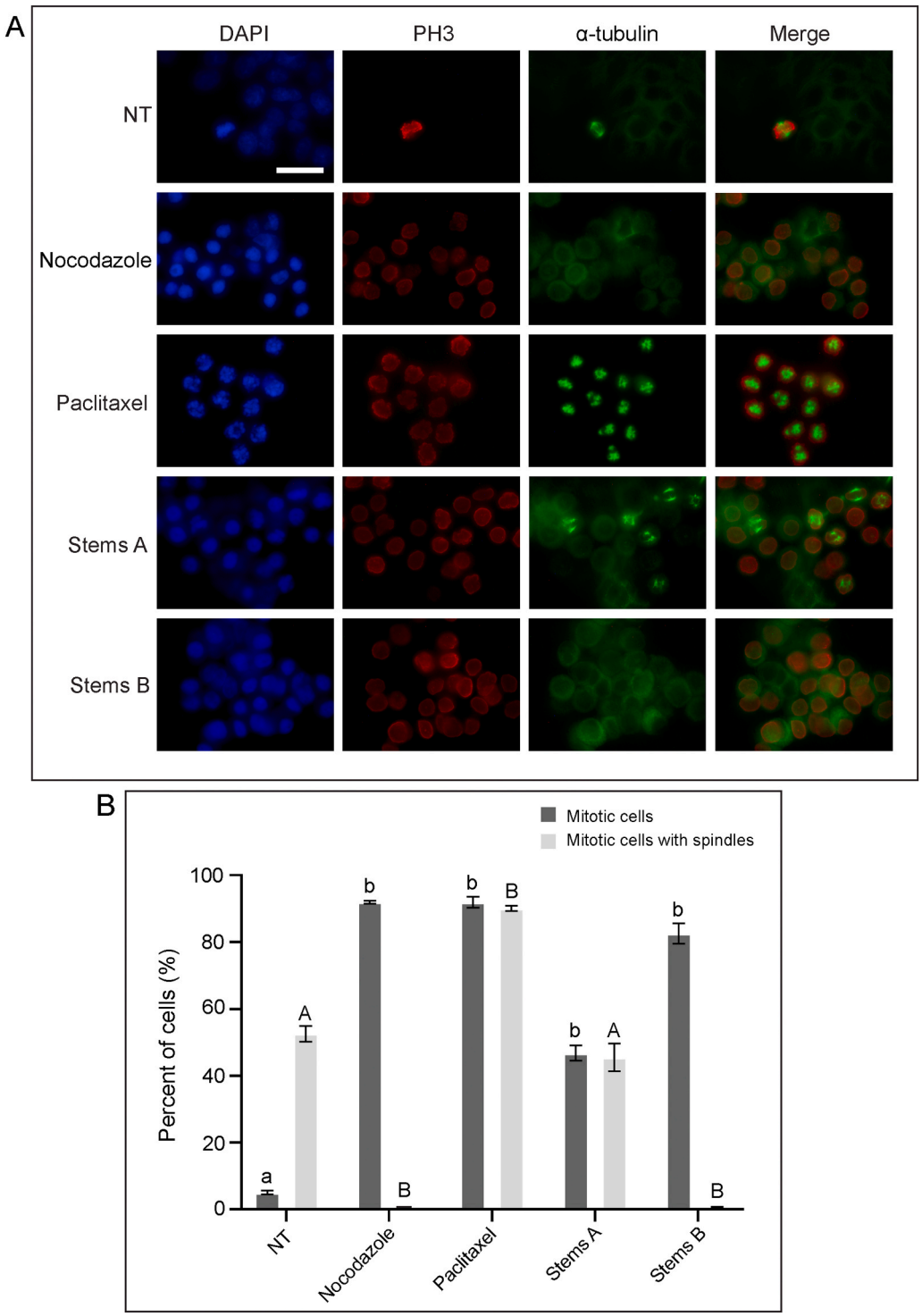

Fig. 4. HT-29 cells treated with stems extracts exhibit a phospho-histone H3 signal with and without mitotic spindles. **A.** HT-29 cells were either not-treated or treated with 500 nM nocodazole, 100 nM paclitaxel, 150 μg/mL stems A or 50 μg/mL stems B extracts for 18 h. Cells were analyzed by immunofluorescence microscopy where DNA was detected with DAPI (blue), phosphorylated histone H3 with anti-phospho-histone H3 antibodies (red), and tubulin with anti-α-tubulin antibodies (green). The merge column is the combination of phospho-histone H3 and α-tubulin staining. Scale bar represents 50 μm. **B.** The mean percentages of cells exhibiting a phospho-histone H3 signal (mitotic cells, dark grey) and mitotic cells with a mitotic spindle (light grey) after treatment. Error bars represent the SEM of at least three independent experiments. Statistical significance was determined using one-way ANOVA followed by Tukey's post hoc test ($p < 0.0001$). Means that are significantly different from the mean of the not-treated control are represented with a different letter (a, b; A, B).

treated cells had high numbers of PH3-positive cells, supporting the evidence that cell rounding was an arrest in mitosis. Close observation of fraction 2-treated cells revealed that 87 ± 1 % of the cells positive for PH3 had a spindle structure, as did cells treated with paclitaxel, albeit the spindle morphologies were different. In contrast, fraction 5-treated cells were PH3-positive but did not display spindles (2 ± 1 %), similar to that of cells treated with nocodazole (Figs. 5C, D) and 4-deoxypodophellotoxin (Supplemental Figure 5). Fraction 3-treated cells

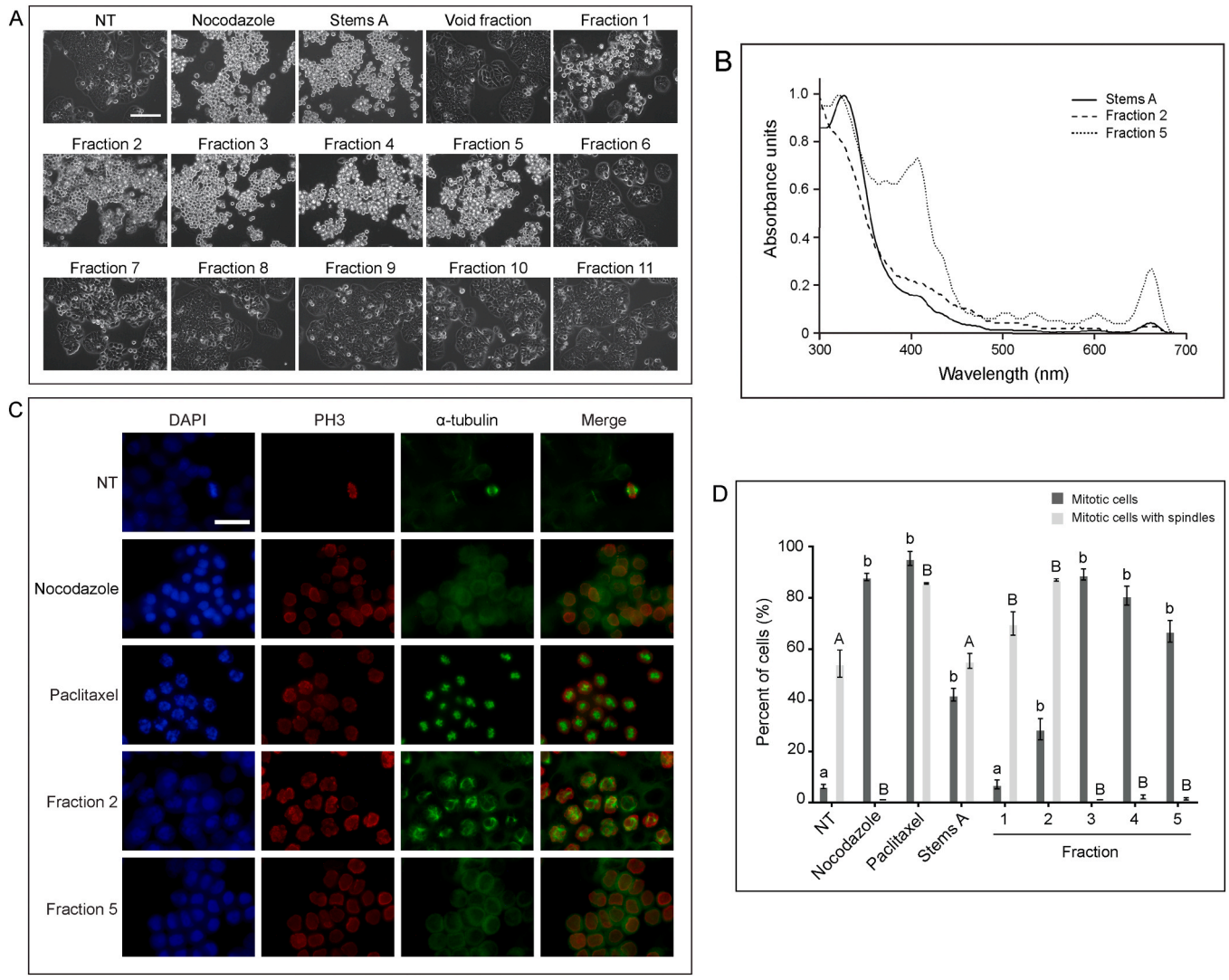

Fig. 5. Fractionation of stems A extract distinguishes the anti-mitotic activities. **A.** HT-29 cells were either not-treated or treated with 500 nM nocodazole, 150 μg/mL stems A, 150 μg/mL fractions 1 through 11, or void fraction for 18 h. Images were taken by light microscopy and representative images are shown. Scale bar represents 100 μm. **B.** UV/visible absorbance spectra of stems A whole extract (solid line), fraction 2 (dashed line) and fraction 5 (dotted line). **C.** HT-29 cells were either not-treated or treated with 500 nM nocodazole, 100 nM paclitaxel, 150 μg/mL stems A, 30 μg/mL fraction 2 or 150 μg/mL fraction 5 for 18 h. Cells were analyzed by immunofluorescence microscopy where DNA was detected with DAPI (blue), phosphorylated histone H3 with anti-phospho-histone H3 antibodies (red), and tubulin with anti-α-tubulin antibodies (green). The merge column is the combination of phospho-histone H3 and α-tubulin staining. Scale bar represents 50 μm. **D.** The mean percentages of cells exhibiting a phospho-histone H3 signal (mitotic cells, dark grey) and mitotic cells with a spindle structure (light grey) after treatment. Error bars represent the SEM of at least three independent experiments. Statistical significance was determined using one-way ANOVA followed by Tukey's post hoc test ($p < 0.005$). Means that are significantly different from the mean of the not-treated control are represented with a different letter (a, b; A, B).

displayed a spindle structure at 10 μg/mL, but spindles were not detected when the concentration was increased to 30 μg/mL, however the PH3 signal was present at both concentrations (Supplemental Figure 5). We concluded that *P. nuttalliana* contains two distinct anti-mitotic activities: one that arrests cells with mitotic spindles and another that arrests cells without spindles.

The two different biological responses (mitotic arrest with spindles and mitotic arrest without spindles) and the elution of these activities into separate fractions by chromatography suggested that this was the result of two distinct compounds. We had previously distinguished anti-mitotic chemical families by including a reduction step in the phenotypic assay [24]. To assess this, we mixed each fraction with the reducing agent beta-mercaptoethanol (β-ME) prior to treatment of cell cultures. In addition, cells were either not-treated or treated with nocodazole in the presence or absence of β-ME. Furthermore, we included two other mitotic-arresting compounds: 4-deoxypodophyllotoxin, which depolymerizes tubulin [31] and is insensitive to β-ME, and hymenoratin, a natural product that induces mitotic arrest with spindles [23] and is sensitive to reduction by β-ME. After 18 h of treatment, the cells were observed by light microscopy (Fig. 6). β-ME did not induce mitosis in not-treated cells, nor did it diminish the cell rounding in nocodazole- or 4-deoxypodophyllotoxin-treated cells. In contrast, β-ME diminished the cell rounding activity of hymenoratin, demonstrating that different types of anti-mitotic compounds can be distinguished in this assay. Importantly, β-ME also diminished the mitotic arrest activity of fraction 2 (mitotic arrest with spindles) but not the mitotic arrest activity of fraction 5 (mitotic arrest without spindles). These data support the conclusion that *P. nuttalliana* harbours two anti-mitotic activities that are both biologically and chemically distinct.

3.3. Isolation of anemonin from Pulsatilla nuttalliana and characterization of mitotic arrest

We used biology guided fractionation to isolate the compound that

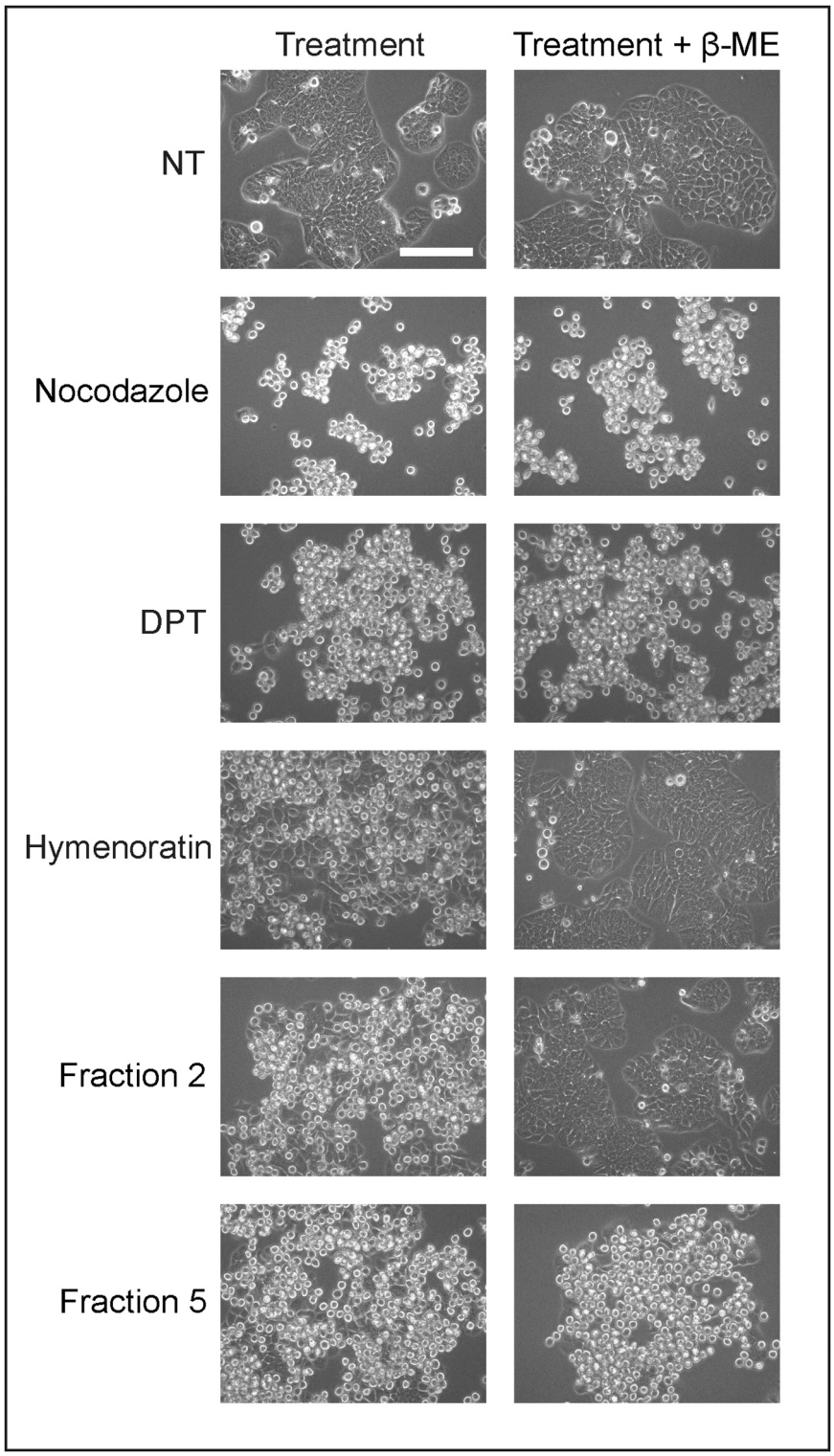

Fig. 6. Cell rounding activity of fraction 2 was diminished after reduction by beta-mercaptoethanol, whereas the cell rounding activity of fraction 5 was maintained. HT-29 cells were either not-treated or treated with 500 nM nocodazole, 50 nM 4-deoxypodophyllotoxin (DPT), 15 μM hymenoratin, 30 μg/mL fraction 2 or 150 μg/mL fraction 5 for 18 h. Treatments were administered either alone or after preincubation with beta-mercaptoethanol (β-ME). Images were taken by light microscopy and representative images are shown. Scale bar represents 100 μm.

induced the mitotic arrest with spindles from *P. nuttalliana* stems. Through successive rounds of fractionation, we isolated anemonin ($C_{10}H_8O_4$) from *P. nuttalliana* (Fig. 7A) and the structure was elucidated by analysis of 1D and 2D NMR data and high-resolution mass spectrometry (supplemental data). The proton and carbon NMR data recorded for the sample in DMSO-d_6 exactly matched the literature values (supplemental data) [30].

We confirmed in cell rounding assays that anemonin induced 44 ± 4 % cell rounding at 15 μM in HT-29 cells which was similar to the effect of fraction 2 which induced 45 ± 3 % cell rounding. An increase in the concentration of anemonin to 50 μM did not increase the percentage of cell rounding (Fig. 7B, C). An independent source of anemonin was

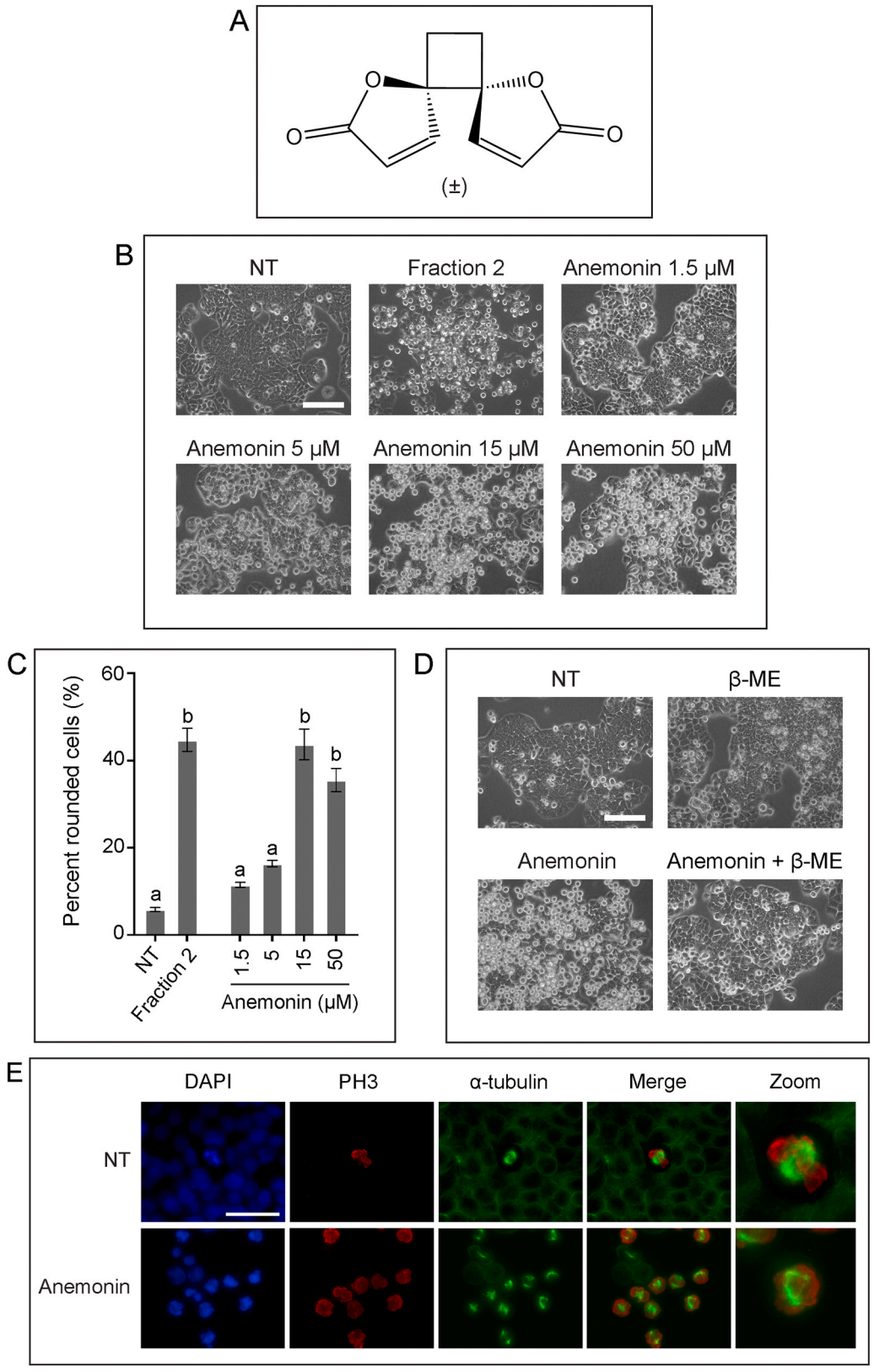

(caption on next page)

Fig. 7. Anemonin, isolated by biology-guided fractionation of *P. nuttalliana*, induced cell rounding in HT-29 cells and its activity can be eliminated by beta-mercaptoethanol reduction. **A.** The structure of anemonin. **B.** HT-29 cells were either not-treated or treated with 30 μg/mL fraction 2 or varying concentrations of anemonin for 18 h. **C.** The mean percentages of cells exhibiting a rounded morphology after treatment. Error bars represent the SEM of at least three independent experiments. Statistical significance was determined using one-way ANOVA followed by Tukey's post hoc test ($p < 0.0001$). Means that are significantly different from the mean of the not-treated control are represented with a different letter (a, b). **D.** HT-29 cells were either not-treated or treated with 15 μM anemonin for 18 h, where treatments were either administered alone or after preincubation with beta-mercaptoethanol (β-ME). Images were taken by light microscopy and representative images are shown. Scale bar represents 100 μm. **E.** HT-29 cells were either not-treated or treated with 15 μM anemonin for 18 h. Cells were analyzed by immunofluorescence microscopy where DNA was detected with DAPI (blue), phosphorylated histone H3 with anti-phospho-histone H3 antibodies (red), and tubulin with anti-α-tubulin antibodies (green). The merge column is the combination of phospho-histone H3 and α-tubulin staining. Scale bar represents 50 μm.

purchased and tested in a separate experiment and induced cell rounding, confirming its activity (data not shown). We then tested whether the cell rounding activity of anemonin could be diminished after incubation with β-ME, as observed in experiments using extract fraction 2. Cells were either not-treated, or treated with β-ME, anemonin, or anemonin that was preincubated with β-ME (Fig. 7D). As we observed with fraction 2, the cell rounding activity of anemonin was diminished by β-ME. Finally, we confirmed that anemonin was the compound responsible for the mitotic arrest with spindle structures by immunofluorescence microscopy (Fig. 7E). These data provided evidence that *P. nuttalliana* harbours two distinct anti-mitotic compounds: one that arrests cells in mitosis without mitotic spindles, and another that arrests cells in mitosis with spindle structures which we identified as the natural product anemonin.

4. Discussion

This study is the first to report two distinct anti-mitotic activities in one botanical species and to identify the anti-mitotic activity of the natural product anemonin. The *Pulsatilla* genus harbours numerous biological activities [32], including inhibition of cancer-related signalling pathways by *P. patens* extracts [33], increased cancer cell death by *P. decoction* extracts [34], inhibition of cell proliferation by pulsatilla saponin D [35] and inhibition of mitosis by deoxypodophyllotoxin [27], both isolated from *P. koreana*. Neither of the two North American species from this genus, *P. nuttalliana* and *P. occidentalis*, a have been investigated previously for biological activity.

Anemonin is a bicyclic butenolide first isolated in 1792 [36] and is a natural product present in species of the Ranunculaceae family, including *P. chinensis* [37], *P. wallichiana* [38], *Clematis chinensis* [39], and now *P. nuttalliana*. It is recognised for its anti-inflammatory activity [40,41] and has been reported to exhibit cytotoxicity against certain cancer cell lines [38,39]. Anemonin, however, has not been previously reported to arrest cells in mitosis. We observed that cells treated with anemonin exhibit cell rounding, a phosphorylated histone H3 signal, and a prolonged mitotic arrest with distorted spindles. This suggests that anemonin inhibits a protein required for mitotic progression. The activity of anemonin in these cell-based assays was similar to those of previously identified sesquiterpene lactones isolated from the Asteraceae botanical family, including hymenoratin [23], pulchelloid A [22], 6-O-angeloylplenolin [42] and psilostachyins A and C [43]. Interestingly, the features of distorted mitotic spindles and sensitivity to reduction by β-ME were also seen in (+)-6-tuliposide A, which we recently identified from *Erythronium grandiflorum* (Liliaceae) [24], suggesting that this anti-mitotic phenotype is not exclusive to sesquiterpene lactones nor exclusive to the Asteraceae family.

The similarity in the biological and chemical responses between these compounds may be due to the shared α,β-unsaturated carbonyl which is the functional group responsible for their biological activity, as demonstrated in structure-activity studies with coronopilin [44] and psilostachyin A [43]. α,β-unsaturated carbonyls react with nucleophiles, such as the cysteine residues found in the reaction centers of some proteins [45–47], and can inhibit the activity of proteins required for mitotic progression. The Ranunculaceae and Asteraceae families diverged over 140 million years ago [48], which presents a phylogenetic distance that may lead to chemical divergence of anti-mitotic compounds. This expands the botanical sources harbouring electrophile functional groups, which may act as Michael acceptors and are sensitive to β-ME. It supports the search for compounds beyond the Asteraceae family to identify similar anti-mitotic phenotypes through phylogenetic bioprospecting, an important tool in drug discovery [49–54].

Based on this rationale, similarities between the anti-mitotic activities of other compounds containing α,β-unsaturated carbonyls should be considered. The natural product 13-hydroxy-15-oxoapatlin (OZ) was found to induce a 30 % mitotic arrest with distorted spindles and misaligned chromosomes, and the researchers proposed that OZ may interact with a motor protein which would inhibit chromosome congression [55]. The natural product *ent*-15-oxokaurenoic acid (EKA) is another example of a compound that induces a 20–30 % mitotic arrest with an abnormal spindle structure [56]. These compounds contain α,β-unsaturated carbonyl groups that have been shown to be required for the anti-mitotic activity of similar compounds since their activity is eliminated when the functional group is reduced [24,43,44]. Identifying novel protein targets with which to inhibit mitosis contributes to the development of new anti-cancer medicines, therefore these distinct mitotic arrest phenotypes warrant further investigation.

The results of the bio-assays and chemical tests for *P. nuttalliana* fraction 5 were consistent with those of a 4-deoxypodophyllotoxin-like activity. 4-deoxypodophyllotoxin (DPT) is an anti-mitotic compound that inhibits microtubule polymerization [31] and has been previously identified in *P. koreana* [27]. β-peltatin, a podophyllotoxin isomer, was recently isolated from *P. decoction* and was found to induce a G2/M cell cycle arrest in pancreatic cancer cell lines [57]. The similarities observed between the no-spindle phenotype of DPT and fraction 5 include similar cell rounding percentages, insensitivity to β-ME, and mitotic arrest without spindles. Further investigation of fraction 5 may reveal that its chemical composition contains podophyllotoxin, β-peltatin, or a related compound characterized to depolymerize tubulin.

It is also noteworthy that the two activities of *P. nuttalliana* could act in parallel (Fig. 4A) suggesting that the two compounds act on different pathways. It is possible that the two distinct activities present in stems A may account for the variability we observed by the MTT cell viability assay (Fig. 3B). We also observed that increasing the concentration of fraction 3 in treated cells resulted in different phenotypes. These results suggest that both activities were present but in different amounts in the sample (Supplemental Figure 5). In future studies, it is possible that phenotypic diversity can be anticipated among the biological activity of secondary metabolites from botanical species in extreme and variable conditions, such as those found in Canadian ecological zones [12].

We report that anemonin is a member of a growing number of natural products that cause mitotic arrest phenotypes with distorted spindles. This emerging group of compounds may help identify novel targets to inhibit mitosis. We identified that one botanical species, *P. nuttalliana,* contains two distinct anti-mitotic activities. Further investigations will include identifying the chemical compound inducing the podophyllotoxin-like activity, followed by the identification of the precise cellular targets for both compounds. Our new data describing the natural product anemonin sets the stage for future mechanistic studies on its anti-mitotic activity. Canadian plant species hold tremendous potential as sources of natural products for advancing our understanding of mitotic regulation and contributing to the development of new medicines.

CRediT authorship contribution statement

Beck Chad R: Investigation. **Layla Molina:** Investigation. **Williams David E:** Methodology, Investigation. **Araba Sagoe-Wagner:** Investigation. **Lockwood Tanner C:** Writing – review & editing, Investigation. **Shannon M Healy Knibb:** Writing – review & editing, Writing – original draft, Investigation, Formal analysis. **Benjamin Yeremy:** Methodology, Investigation. **Golsteyn Roy M:** Writing – review & editing, Supervision, Investigation, Funding acquisition, Conceptualization. **Andersen Raymond J:** Writing – review & editing, Supervision, Funding acquisition, Conceptualization.

Funding

This work was supported by Discovery Grants from the Natural Sciences and Engineering Council of Canada (NSERC) to RMG and RJA, and the Monaghan Prairie to Pharmacy Fund to RMG.

Declaration of Competing Interests

The authors declare that they have no known competing financial interests or personal relationships that could have appeared to influence the work reported in this paper.

Acknowledgements

We thank Dr. Sophie Kernéis (Lethbridge Polytechnic) and members of the Natural Product Laboratory for valuable discussions. We thank the following organizations and people for granting permission to collect plants on public or private lands: Michelle Armstrong (Alberta Environment and Parks), Alberta Tourism Parks and Recreation, City of Lethbridge, and the Monaghan family.

Appendix A. Supporting information

Supplementary data associated with this article can be found in the online version at doi:10.1016/j.prenap.2025.100361.

Data availability

Data will be made available on request.

References

[1] P.B. Schiff, J. Fant, S.B. Horwitz, Promotion of microtubule assembly in vitro by taxol, Nature 277 (1979) 665–667.
[2] M.C. Wani, et al., The isolation and structure of taxol, a novel antileukemic and antitumor from taxus brevifolia, Am. Chem. Soc. 93 (1971) 2325–2327.
[3] G.M. Cragg, Paclitaxel (Taxol): a success story with valuable lessons for natural product drug discovery and development, Med. Res. Rev. 18 (1998) 315–331.
[4] J. Gallego-Jara, et al., A compressive review about taxol: history and future challenges, Molecules 25 (2020) 5986–6010.
[5] D.G.I. Kingston, My 60-year love affair with natural products, J. Nat. Prod. 84 (2021) 932–948.
[6] C.C. Thornburg, et al., NCI program for natural product discovery: a publicly-accessible library of natural product fractions for high-throughput screening, Am. Chem. Soc. Chem. Biol. 13 (2018) 2484–2497.
[7] L. Molina, et al., Connecting plant species and natural products from the Canadian prairie ecological zone to biomedical knowledge, Botany 100 (2022) 231–245.
[8] B.A.P. Wilson, et al., Creating and screening natural product libraries, Nat. Prod. Rep. 37 (2020) 893–918.
[9] T. Hartmann, Diversity and variability of plant secondary metabolism: a mechanistic view, Èntomol. Exp. Et. Appl. 80 (1996) 177–188.
[10] D.P. Pavarini, et al., Exogenous influences on plant secondary metabolite levels, Anim. Feed Sci. Technol. 176 (2012) 5–16.
[11] F.T. Maestre, et al., Grazing and ecosystem service delivery in global drylands, Science 378 (2022) 915–920.
[12] N. Gross, et al., Unforeseen plant phenotypic diversity in a dry and grazed world, Nature 632 (2024) 808–814.
[13] L. Kershaw, L. Allen, 2020, Vascular Flora of Alberta: An illustrated guide.
[14] D.C. Swinney, J. Anthony, How were new medicines discovered? Nat. Rev. Drug Discov. 10 (2011) 507–519.
[15] D.E. Williams, R.J. Andersen, Biologically active marine natural products and their molecular targets discovered using a chemical genetic approach, Nat. Prod. Rep. 37 (2020) 617–633.
[16] F.M. Perron-Sierra, et al., Synthesis of cis-fused pyran indolocarbazole derivatives that inhibit FLT3 kinase and the DNA damage kinase, checkpoint kinase 1, AntiCancer Agents Med. Chem. 12 (2012) 194–201.
[17] J.G. Moffat, et al., Opportunities and challenges in phenotypic drug discovery: an industry perspective, Nat. Rev. Drug Discov. 16 (2017) 531–543.
[18] K.E. Gascoigne, S.S. Taylor, Cancer cells display profound intra- and interline variation following prolonged exposure to antimitotic drugs, Cancer Cell 14 (2008) 111–122.
[19] P.M. Kubara, et al., Human cells enter mitosis with damaged DNA after treatment with pharmacological concentrations of genotoxic agents, Biochem. J. 446 (2012) 373–381.
[20] L.H. Swift, R.M. Golsteyn, Experimental determination of checkpoint adaptation by mitotic shake-off and microscopy, Methods Mol. Biol. 1769 (2018) 159–168.
[21] A. Bosco, R.M. Golsteyn, Emerging anti-mitotic activities and other bioactivities of sesquiterpene compounds upon human cells, Molecules 22 (2017) 459–481.
[22] A. Bosco, et al., Pulchelloid A, a sesquiterpene lactone from the Canadian prairie plant gaillardia aristata inhibits mitosis in human cells, Mol. Biol. Rep. 48 (2021) 5459–5471.
[23] L. Molina, et al., Isolation of a natural product with anti-mitotic activity from a toxic Canadian prairie plant, Heliyon 7 (2021) e07131.
[24] S.M. Healy Knibb, et al., An anti-mitotic compound, (+)-6-tuliposide A, isolated from the Canadian glacier lily, erythronium grandiflorum, Fitoterapia 177 (2024) 106075.
[25] E. Beaubien, A. Hamann, Spring flowering response to climate change between 1936 and 2006 in alberta, Canada, BioScience 61 (2011) 514–524.
[26] B.H. Park, et al., Antitumor activity of pulsatilla koreana extract in anaplastic thyroid cancer via apoptosis and anti-angiogenesis, Mol. Med. Rep. 7 (2013) 26–30.
[27] Y. Kim, et al., Deoxypodophyllotoxin: the cytotoxic and antiangiogenic component from pulsatilla koreana, Planta Med. 68 (2002) 271–274.
[28] E.H. Moss, J.G. Packer, Flora of alberta: a manual of flowering plants, conifers, ferns, and fern allies found growing without cultivation in the province of alberta, University of Toronto Press, *Canada*, 1983.
[29] C.W. Lewis, R.M. Golsteyn, Cancer cells that survive checkpoint adaptation contain micronuclei that harbor damaged DNA, Cell Cycle 15 (2016) 3131–3145.
[30] R. Saidi, et al., Tunisian clematis flammula essential oil enhances wound healing: GC-MS analysis, biochemical and histological assessment, J. Oleo Sci. 67 (2018) 1483–1499.
[31] S. Desbène, S. Giorgi-Renault, Drugs that inhibit tubulin polymerization: the particular case of podophyllotoxin and analogues, Curr. Med. Chem. 2 (2002) 71–90.
[32] G. Łaska, et al., Phytochemical screening of pulsatilla species and investigation of their biological activities, Acta Soc. Bot. Pol. 88 (2019) 3613.
[33] G. Łaska, et al., Extracts from pulsatilla patens target cancer-related signaling pathways in HeLa cells, Sci. Rep. 11 (2021) 10654–10670.
[34] Y. Jie, X. Yang, W. Chen, Pulsatilla decoction combined with 5-fluorouracil triggers immunogenic cell death in the colorectal cancer cells, Cancer Biotherapy Radiopharm. 37 (2022) 945–954.
[35] M.K. Son, et al., SB365, pulsatilla saponin d suppresses the proliferation of human colon cancer cells and induces apoptosis by modulating the AKT/mTOR signalling pathway, Food Chem. 136 (2013) 26–33.
[36] R.M. Moriarty, et al., The structure of anemonin, J. Am. Chem. Soc. 87 (1965) 3251–3252.
[37] H. Duan, et al., Effect of anemonin on NO, ET-1 and ICAM-1 production in rat intestinal microvascular endothelial cells, J. Ethnopharmacol. 104 (2006) 362–366.
[38] I. Ali, et al., Isolation of anemonin from pulsatilla wallichiana and its biological activities, J. Chem. Soc. Pak. 41 (2019) 325–333.
[39] Y.H. Huang, et al., Anemonin is a natural bioactive compound that can regulate tyrosinase-related proteins and mRNA in human melanocytes, J. Dermatol. Sci. 49 (2008) 115–123.
[40] L. Jiang, et al., Anti-inflammatory effects of anemonin on acute ulcerative colitis via targeted regulation of protein kinase C-θ, Chin. Med. 17 (2022) 39–51.
[41] Z. Wang, et al., Anemonin attenuates osteoarthritis progression through inhibiting the activation of the IL-1B/NF-κB pathway, J. Cell. Mol. Med. 21 (2017) 3231–3243.
[42] Y. Liu, et al., Small compound 6-O-angeloylplenolin induces mitotic arrest and exhibits therapeutic potentials in multiple myeloma, Public Libr. Sci. One 6 (2011) e21930.
[43] C.M. Sturgeon, et al., Modulation of the G2 cell cycle checkpoint by sesquiterpene lactones psilostachyins a and c isolated from the common ragweed ambrosia artemisiifolia, Planta Med. 71 (2005) 938–943.
[44] R. Cotugno, et al., Effect of sesquiterpene lactone coronopilin on leukaemia cell population growth, cell type-specific induction of apoptosis and mitotic catastrophe, Cell Prolif. 45 (2012) 53–65.
[45] D.W. Bak, et al., Cysteine reactivity across the subcellular universe, Curr. Opin. Chem. Biol. 48 (2019) 96–105.
[46] C.A. Berdan, et al., Parthenolide covalently targets and inhibits focal adhesion kinase in breast cancer cells, Cell Chem. Biol. 26 (2019) 1027–1035.
[47] P.A. Jackson, et al., Covalent modifiers: a chemical perspective on the reactivity of alpha,beta-unsaturated carbonyls with thiols via hetero-michael addition reactions, J. Med. Chem. 60 (2017) 839–885.

[48] N. Wikström, V. Savolainen, M.W. Chase, Evolution of the angiosperms: calibrating the family tree, Proc. R. Soc. Lond. 268 (2001) 2211–2220.
[49] M.G.K. Bay-Smidt, et al., Phylogenetic selection of target species in amaryllidaceae tribe haemantheae for acetylcholinesterase inhibition and affinity to the serotonin reuptake transport protein, South Afr. J. Bot. 77 (2011) 175–183.
[50] E.J. Culp, et al., Evolution-guided discovery of antibiotics that inhibit peptidoglycan remodelling, Nature 578 (2020) 582–587.
[51] E. Guzman, J. Molina, The predictive utility of the plant phylogeny in identifying sources of cardiovascular drugs, Pharm. Biol. 56 (2018) 154–164.
[52] M.M. Larsen, et al., Using a phylogenetic approach to selection of target plants in drug discovery of acetylcholinesterase inhibiting alkaloids in amaryllidaceae tribe galantheae, Biochem. Syst. Ecol. 38 (2010) 1026–1034.
[53] D. Liana, K. Rungsihirunrat, Phytochemical screening, antimalarial activities, and genetic relationship of 16 indigenous Thai asteraceae medicinal plants: a combinatorial approach using phylogeny and ethnobotanical bioprospecting in antimalarial drug discovery, J. Adv. Pharm. Technol. Res. 12 (2021) 254–260.
[54] J. Pellicer, et al., A phylogenetic road map to antimalarial artemisia species, J. Ethnopharmacol. 225 (2018) 1–9.
[55] N.T. Rundle, et al., G2 DNA damage checkpoint inhibition and antimitotic activity of 13-hydroxy-15-oxozoapatlin, J. Biol. Chem. 276 (2001) 48231–48236.
[56] N.T. Rundle, et al., An ent-kaurene that inhibits mitotic chromosomes movement and binds the kinetochore protein ran-binding protein 2, Am. Chem. Soc. Chem. Biol. 1 (2006) 443–450.
[57] R. Wu, et al., Pulsatilla decoction and its bioactive component beta-peltatin induce G2/M cell cycle arrest and apoptosis in pancreatic cancer, Chin. Med. 18 (2023) 61–74.